



OPEN ACCESS

EDITED BY

Jianyong Han,
Shandong Jianzhu University, China

REVIEWED BY

Hongzhan Cheng,
Hunan University, China
Wengang Dang,
National Sun Yat-sen University, Taiwan

*CORRESPONDENCE

Lu Bai,
✉ lu.bai@chnenergy.com.cn

RECEIVED 23 October 2023

ACCEPTED 06 November 2023

PUBLISHED 28 December 2023

CITATION

Zou J, Wang M, Bai L and Yan C (2023),
Numerical study on migration of
overlying strata and propagation of
cracks during multi-coal seams mining.
Front. Earth Sci. 11:1326597.
doi: 10.3389/feart.2023.1326597

COPYRIGHT

© 2023 Zou, Wang, Bai and Yan. This is an
open-access article distributed under the
terms of the [Creative Commons
Attribution License \(CC BY\)](https://creativecommons.org/licenses/by/4.0/). The use,
distribution or reproduction in other
forums is permitted, provided the original
author(s) and the copyright owner(s) are
credited and that the original publication
in this journal is cited, in accordance with
accepted academic practice. No use,
distribution or reproduction is permitted
which does not comply with these terms.

Numerical study on migration of overlying strata and propagation of cracks during multi-coal seams mining

Junpeng Zou¹, Man Wang², Lu Bai^{1*} and Chongwei Yan³

¹State Key Laboratory of Water Resource Protection and Utilization in Coal Mining, Beijing, China, ²College of Information Engineering, Wuhan Business University, Wuhan, China, ³Faculty of Engineering, China University of Geosciences, Wuhan, China

The surface subsidence caused by the coal seam mining seriously affects the ecology of the mining area. Compared with the single-coal seam mining, the mechanism of the overburden fracture and crack propagation caused by multi-coal seams mining is more complex, which has not been fully understood. Taking the 22,108 and 42,108 working faces of Buertai Coal Mine as a research object, the discrete element method is used to simulate the migration and failure characteristics of overlying strata, and the propagation of cracks in the process of multi-coal seams mining is also been investigated. So many cracks develop in the soft strata overlying the coal seam, and they cross each other and form a complex fracture system. The hard layer produces staggered cracks with a large size, mainly high-angle longitudinal cracks. The surface subsidence curve of the single coal seam mining shows a wide and slow “bowl” type, and the surface subsidence curve of the double coal seams mining show a “funnel” type with only one inflection point. The overburden structure disturbance caused by the previous coal seam and rock cracking—settlement have great influence on the mining of the latter coal seam. The research results are basically consistent with the field data comparison, which could provide a reference for the related research and engineering practice of shallow-buried double coal seam mining.

KEYWORDS

multi-coal seams mining, overlying strata migration, ground cracks, surface subsidence, particle flow code

1 Introduction

Repeated mining refers to a mining method in which rock strata and surface have been affected by one mining, resulting in movement, deformation, and destruction, and then affected by another mining, causing rock strata and surface to be destroyed again (Liu et al., 2022). In general, the initial mining will damage the overlying rock and cause the softening of rock masses resulting in a decrease in rock mass strength (Zhang et al., 2023a). During the secondary mining, the insufficient amount of damage in the upper coal seam mining will be “activated,” therefore, the damage degree of repeated mining is greater than that of initial mining on rock and surface. To ensure safe production and better direct production, it is necessary to conduct in-depth research on repeated mining.

In recent years, aiming at the characteristics of overlying strata movement caused by single mining in shallow coal seams, scholars have accumulated a lot of practical experience and theoretical basis. However, for multi-seam mining, the overlying strata have been

disturbed to form gob area, the mechanical properties of rock have changed after damage, and the overburden stress is redistributed. The mechanical environment of the mine under the condition of multi-coal seam mining is greatly changed compared with that of shallow coal seam mining, the temporal-spatial evolution law of overlying rock mass and surface deformation is different from that of single coal seam mining. Therefore, the failure characteristics of multi-coal seam mining are quite different from single mining (Yu et al., 2016; Ghabraie et al., 2017a; Ghabraie et al., 2017b; Zhang et al., 2018; Ma and Hu, 2013). By assuming that the reduction of the expansion coefficient of the rock mass during the mining of multiple coal seams is proportional to the amount of expansion caused by the initial mining, combined with the field-measured data, the calculation formula for predicting the subsidence coefficient of the surface and rock mass under the mining conditions of multiple coal seams is given. The simulation study on the development law of overburden fracture under repeated mining conditions is carried out, and it is considered that repeated mining may cause the re-development of the water-conducting fractured zone of the upper coal seam (Yao et al., 2010). Zou et al. (2022a) studied the characteristics of mine tremor and stress distribution before and after deep hole blasting in the mining process of Dongtan Coal Mine in Shandong Province, and revealed the prevention and control effect of deep hole blasting on strong mine tremor. It is considered that deep hole blasting technology can effectively weaken and break the thick and hard rock strata overlying the coal seam, so as to achieve the purpose of releasing the strain energy of the overlying rock (Zou et al., 2022a). The surface and rock mass deformation characteristics under repeated mining conditions were analyzed by FLAC3D numerical simulation software. Based on the key strata theory of strata movement and mine earthquake monitoring technology, the collaborative migration and fracture characteristics of multi-key strata in deep coal mining and the energy propagation law of induced mine earthquakes were studied (Zhang et al., 2023b). Through on-the-spot observation and theoretical analysis of the working face of close distance thick coal seam group in 7 and 8 coal seams in the Datun mining area, it is concluded that the height of the lower coal falling zone increases when the failure range of the upper coal floor coincides with the development range of lower coal falling zone. Using numerical simulation, similar simulation, and engineering practice, the range of the shear fracture zone and stress concentration area near the working face is defined. Based on digital image correlation technology and traditional split Hopkinson pressure bar test, Zou et al. (2022b) conducted a series of repeated experiments on complete, rough and smooth joint surfaces, and described the process of stress wave propagation through joints in rock mass. The instability law of the damaged basic roof is studied based on the “S-R” theory of the “Vousoir beam structure.” It is concluded that the damaged basic roof is more prone to sliding instability of the “Vousoir beam.” and the greater the damage, the greater the probability of sliding instability (He et al., 2016). The hypothesis of “Vousoir beam” is proposed based on the characteristics of mining rock mass movement. With the advance of the working face, the hard rock above the goaf will be fractured into orderly rock blocks in the fracture zone, and the rock blocks will be hinged by horizontal thrust. Wei et al. (2022) analyzed the macroscopic and microscopic characteristics of overburden

failure, fracture development, force chain evolution and rock mass damage law through UAV remote sensing technology, laboratory test and PFC2D numerical simulation, and compared them with field data. Based on the actual situation of 22,307 working face in Bulianta Coal Mine, Liu et al. studied the redevelopment of cracks and the change of permeability in the process of lower coal seam mining by using Particle Flow Code and corresponding physical experiments. The results show that after the lower coal seam mining, the upper and lower stopes are connected to form a new compound minefield; with the mining of the lower coal seam and the advancement of the working face, the permeability and the number of cracks in each area of the overlying strata show the law of ‘stability-rapid increase-stability’ (Liu et al., 2019a; Liu et al., 2019b). Based on the BBR research system, Wang et al. (2020) used PFC numerical calculation and a top-coal caving experiment to study the top-coal caving mechanism of sublevel caving in steeply inclined coal seams under different sublevel heights and caving directions. The results show that the boundary curve of top coal can be fitted by a parabola. Like a flat coal seam, the drainage body of SLTCC is still a cutting variational ellipsoid. With the increase of the section height, the convex point of the top coal boundary moves to the goaf, which leads to the incomplete development of the top coal (Wang et al., 2020). Aiming at the problems of high gas concentration in overlying strata and uncertain roof height in the 7,435 working face of Kongzhuang Coal Mine, Wang et al. (2017) studied the caving characteristics of overlying strata by combining physical experiments of similar materials with numerical simulation of PFC (Particle Flow Code) software and verified each other. The relationship between fracture development and porosity variation characteristics is introduced to quantitatively determine the height of the local fracture zone. The quantitatively calculated wellbore height is compared with the wellbore height measured by the *in situ* drilling flow method (Wang et al., 2017). In order to study the strength behavior of coal pillars under different confining stresses, Zhang et al. carried out compressive tests under lateral constraints of 0~8.0 MPa, and the PFC model to study the strength enhancement mechanism of coal pillars at the particle scale. It is concluded that the strength and cumulative axial strain of coal increase with the increase of constraint, while Young’s modulus is independent of constraint. Compared with the significant increase of peak compressive stress, the crack initiation stress increases slightly with the increase of constraint. In the early stage of loading, the high constraint inhibits the development of microcracks, while in the later stage of loading, the high constraint enhances the frictional resistance strength component. These two mechanisms together change the compressive strength of coal, which helps to mobilize the strength component (Zhang and Li, 2019). With the continuous development of measurement technology, a large number of scholars continue to apply new technologies to multi-seam mining surface deformation monitoring and achieved a series of results (Perski et al., 2009; Ge L. et al., 2007; Jung et al., 2007; Baek et al., 2008; Wu et al., 2008; Y et al., 2008).

The surface subsidence law and fracture propagation mechanism induced by multi-coal seam mining have been deeply studied by numerical simulation, field observation, laboratory test, and theoretical analysis. However, the research on the mechanism of repeated disturbance of lower coal seam mining to upper coal seam

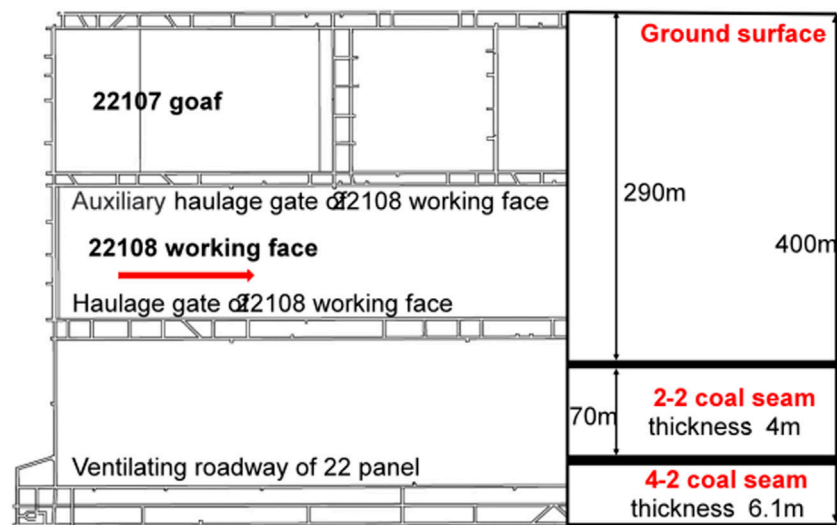


FIGURE 1
Roadway layout of 22,108 working face and the positional relationship between 2-2 and 4-2 coal seams.

goaf is still insufficient. This paper takes the 22,108 and 42,108 working face of the Buertai mining area as an example, PFC numerical simulation software is used to study the characteristics of surface subsidence and fracture propagation under the condition of double-layer downward mining, revealing the mutual feedback mechanism of strata movement law caused by upper and lower coal seam mining, to contribute to the study of overburden rock migration mechanism induced by multi-coal seam mining.

2 Engineering background

Buertai coal mine is located in Ordos city, inner Mongolia Autonomous Region. It is a super large production mine of Shenhua Coal Group Co., Ltd. The coal mine is designed in 2005, with a design production capacity of 20 million tons/year. Construction began in 2008, trial production in 2011, and production in 2014. The main mining 22 coal and 42 coal seam are extracted with the mechanized longwall retreat method, all falling method to deal with gob roof. This paper studies the 22,108 working face of the 2-2 coal seam and the 42,108 working face of the 4-2 coal seam. The compressive strength of the rock in the natural state of Buertai Coal Mine is relatively low, basically below 40 Mpa. The shear and tensile strength are relatively high, and the softening coefficient of the rock is mostly less than 0.75, all of which are softened rock. In general, the roof and floor rocks of coal seams in this area are mainly weak rocks, followed by semi-hard rocks.

Forty-two thousand one hundred and eight working face is the eighth working face of 42 coal seam, the width of 42,108 working face is 300.2 m and the mining length is 4,728.4 m, and the thickness of the overlying loose layer is 1~40 m. The average thickness of the coal seam is 6.1 m, the dip angle is $1^{\circ}\sim 3^{\circ}$, and the average buried depth is 360 m. The immediate roof of 42,108 working face is mostly sandy mudstone, partly mudstone and siltstone. The thickness of the immediate roof is 1~21 m, and the roof is easy to fall or separated

strata. The 42,108 working face is north-south, and the east side is the 42,107 gob area. The width of the 22,108 working face is 300 m, and the stopping length is 4,724.7 m. The average thickness of the coal seam is 4 m, the dip angle is $1^{\circ}\sim 2^{\circ}$, and the average buried depth is 290 m. The direct roof of the 22,108 working face is also dominated by sandy mudstone, and the thickness of the immediate roof is large. The position relationship of the working face is shown in Figure 1, and the physical and mechanical properties of the coal measures strata are shown in Table 1. All parameters are obtained by field exploration and experimental tests.

3 Numerical simulation

PFC2D follows Newton's second law and force-displacement law to simulate the contact, motion, and interaction between particles. The contact force between particles is updated by the force-displacement law, and the position of particles and boundary is sought by Newton's law of motion to form a new contact. The linear parallel bond model is used in this paper, the particles form a whole through bonding contact and can withstand tension, pressure, and torsion within a certain range, contact between particles is broken beyond the range and degenerates into a linear model that only works under pressure. The model can realistically simulate the formation process of roof fracture and hinged structure in the mining process (Cho N. et al., 2007). The mechanical behavior of the linear parallel bond model is shown in Figure 2.

According to the actual distribution of overlying strata in 42,108 working faces, a 2D numerical model of double-layer mining is established. The length of the numerical model is 800 m and the height is 400 m. The minimum particle size is 0.4, the particle size ratio is 1.6, and a total of 321,569 particles are generated. The model's left and right and bottom boundaries are fixed, and the top is a free boundary, as shown in Figure 3. Displacement constraints are set on the left and right sides of the

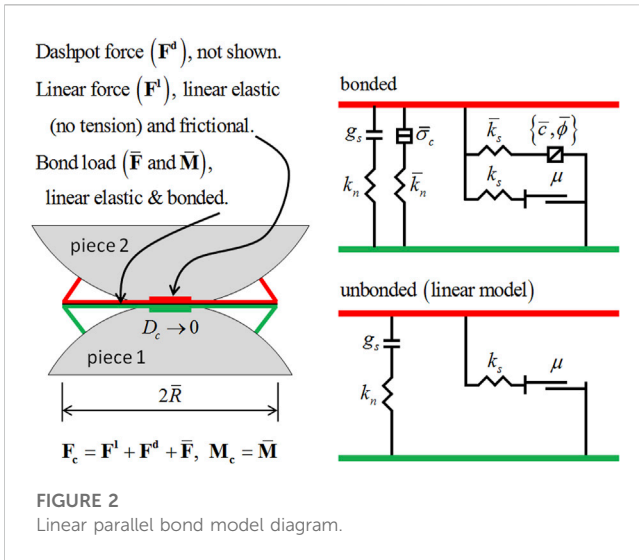
TABLE 1 Physical and mechanical properties of coal and rock masses.

No.	Lithology	Density (kg/m ³)	Thickness (m)	Elasticity modulus (GPa)	Tensile strength (MPa)	Compressive strength (MPa)
1	Loess layer	1,600	12.72	0.12	0.03	0.33
2	Fine sandstone	2,280	20.97	0.6	0.89	11.2
3	Sandy mudstone	2,430	13.27	1.0	20	1.97
4	Medium sandstone	2,230	14.36	0.5	0.55	7.2
5	Coarse conglomerate	1800	20.64	1.5	0.92	12.3
6	Fine sandstone	2,280	15.5	0.6	0.89	11.2
7	Medium sandstone	2,230	20.03	0.5	0.55	7.2
8	Sandy mudstone	2,430	11.67	1.0	20	1.97
9	Medium sandstone	2,230	10.4	0.5	0.55	7.2
10	Fine sandstone	2,280	11.4	0.6	0.89	11.2
11	Sandy mudstone	2,430	20.1	1.0	20	1.97
12	Medium sandstone	2,230	13	0.5	0.55	7.2
13	Sandy mudstone	2,430	11.74	1.0	20	1.97
14	Medium sandstone	2,230	12.16	0.5	0.55	7.2
15	Sandy mudstone	2,430	11.18	1.0	20	1.97
16	Fine sandstone	2,280	16.43	0.6	0.89	11.2
17	Medium sandstone	2,230	15.49	0.5	0.55	7.2
18	Sandy mudstone	2,430	12	1.0	20	1.97
19	Fine sandstone	2,280	12.25	0.6	0.89	11.2
20	Sandy mudstone	2,430	9.93	1.0	20	1.97
21	2-2 coal seam	1,310	4	1.0	0.55	7.2
22	Mudstone	2,400	5.38	2.6	4.3	38
23	Fine sandstone	2,280	7.17	0.6	0.89	11.2
24	Sandy mudstone	2,430	6.63	1.0	20	1.97
25	Siltstone	2,380	11.24	2.0	1.97	16.5
26	Medium sandstone	2,230	5.1	0.5	0.55	7.2
27	Siltstone	2,380	14.57	2.0	1.97	16.5
28	Medium sandstone	2,230	8.39	0.5	0.55	7.2
29	Sandy mudstone	2,430	8.91	1.0	20	1.97
30	4-2 coal seam	1,310	6	1.0	0.55	7.2
31	Mudstone	2,400	20.07	2.6	4.3	38
32	Siltstone	2,380	17.3	2.0	1.97	16.5

model and the bottom boundary, and free boundary condition is set up on the top. The Mohr-Coulomb constitutive model is adopted.

The model considers 32 representative strata according to the drilling data, and the microscopic parameters of each rock layer are shown in Table 2. Before numerical calculation, we need to correct

the microscopic parameters of the model according to the actual mechanical parameters of rock mass. Table 2 shows the corrected parameters. The mining height of the upper and lower coal seams is 4 and 6 m respectively, and the advancing distance of the working face is 300 m. Each working face is excavated 30 times, 10 m each time. To eliminate the influence of the boundary effect on the model,



250 m boundaries are generated on both sides of the model. This research focuses on the characteristics and laws governing overburden and surface damage, omitting the temporary support effect of powered support in the working face.

4 Result in analysis

4.1 Analysis of mining overburden failure and fracture development law

As the first mining proceeds, the immediate roof gradually bends downward to produce separation, and the basic roof cracks develop. As shown in Figure 4, when advancing to 70 m, the immediate roof breaks for the first time, and the basic roof S1 forms a penetrating crack at the position of the cut-off and the working face. When advancing to 90 m, the basic roof S1 is broken, showing the form of a “Voussoir beam” structure, accompanied by separation, and the cracks in the upper middle sandstone soft rock layer of the basic roof S2 develop from both sides of the goaf to the middle. When advancing to

130 m, the basic roof S1 collapsed and the working face is first roof pressure, the central part of the falling zone gradually compacted, and the height of the falling zone is 21 m. The cracks in the S2 cut-off of the basic roof penetrated, and the cracks in the overlying weak medium sandstone layer gradually developed. The basic roof S1 repeats the failure process of “breaking-collapse-compaction.” The falling zone only expands horizontally and no longer develops upward.

When the working face advances to 200 and 280 m respectively, the basic roof S2 forms penetrating cracks from the working face, resulting in a certain degree of damage. However, due to the small thickness of the first coal seam, and the large thickness of the basic roof, resulting in a high backfilling height of the gob area, the basic roof S2 does not collapse. When advancing to 300 m, the numerical simulation mining is completed, the gob area is compacted, the interlayer separation layer is basically closed, and the basic roof S2 exists in the form of a “Voussoir beam” structure with bearing capacity. Affected by the goaf, a large number of cracks are developed in the overlying weak rock layer. In the whole first mining process, there is no obvious bending separation phenomenon in the high overlying strata. The height of the water-conducting fractured zone is 65.1 m, the height of the falling zone is 21 m, and the ratio of mining to falling is 1:5, which is basically consistent with the conclusions of the empirical Eqs 1, 2 of “falling height” and “two-zone” height of medium hard rock strata studied by Liu Shiqi (Liu, 2016).

$$H_m = 4.73M + 4.40 \quad (1)$$

$$H_1 = \frac{100M}{0.23M + 6.1} \pm 10.42 \quad (2)$$

In the formula: H_m is the height of the caving zone; M is the coal seam mining height; H_1 is the height of the water-conducting fractured zone.

Similar to the first mining, as the working face advances, the hard roof R1 gradually bends. As shown in Figure 5, when the working face advances to 70 m, the bending, and sinking of the hard roof R1 are very obvious, and cracks are generated from the cut-off, accompanied by small separation layers, but not broken. When advancing to 100 m, as the subsidence space increases, the roof R1 breaks for the first time, the working face is first roof

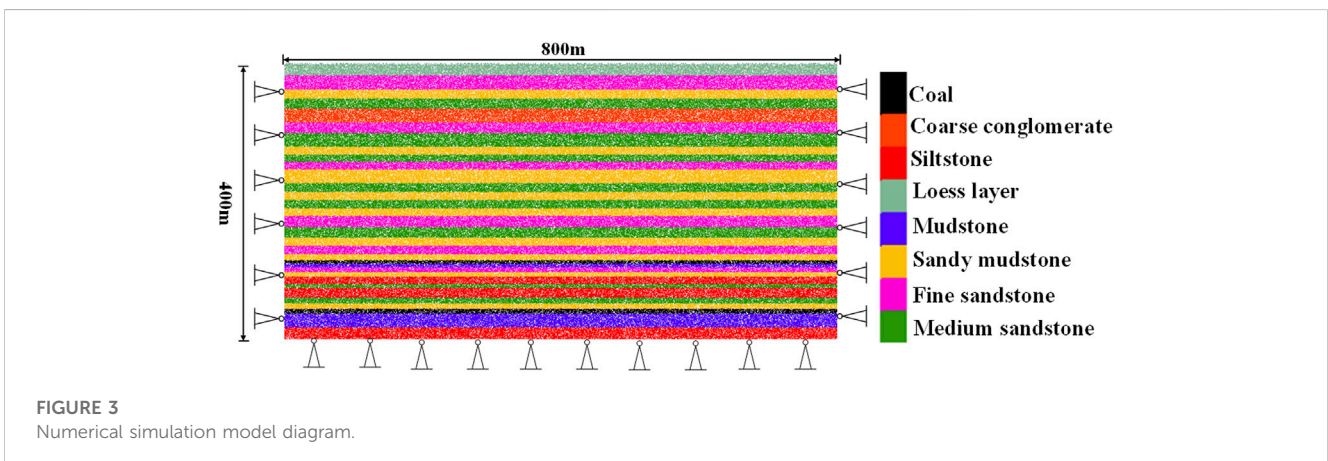


TABLE 2 Microscopic parameters of overburdened rock.

Lithology	σ_c	σ_t	E^*	f_a	f	k
Loess layer	0.2	0.6	0.06	38	0.4	2
Fine sandstone	2.0	3.8	0.3	40	0.3	2
Sandy mudstone	5.0	9	0.5	43	0.3	2
Medium sandstone	1.0	2.7	0.25	43	0.3	2
Coarse conglomerate	1.9	3.7	0.75	42	0.4	2
Fine sandstone	2.0	3.8	0.3	40	0.3	2
Medium sandstone	1.0	2.7	0.25	43	0.3	2
Sandy mudstone	5.0	9	0.5	43	0.3	2
Medium sandstone	1.0	2.7	0.25	43	0.3	2
Fine sandstone	2.0	3.8	0.3	40	0.3	2
Sandy mudstone	5.0	9	0.5	43	0.3	2
Medium sandstone	1.0	2.7	0.25	43	0.3	2
Sandy mudstone	5.0	9	0.5	43	0.3	2
Medium sandstone	1.0	2.7	0.25	43	0.3	2
Sandy mudstone	5.0	9	0.5	43	0.3	2
Fine sandstone	2.0	3.8	0.3	40	0.3	2
Medium sandstone	1.0	2.7	0.25	43	0.3	2
Sandy mudstone (Basic roof S2)	5.0	9	0.5	43	0.3	2
Fine sandstone (Basic roof S1)	2.0	3.8	0.3	40	0.3	2
Sandy mudstone	5.0	9	0.5	43	0.3	2
2-2 coal seam	1.0	2.7	0.5	39	0.3	2
Mudstone	10	27	1.3	38	0.4	2
Fine sandstone	2.0	3.8	0.3	40	0.3	2
Sandy mudstone	5.0	9	0.5	43	0.3	2
Siltstone (Hard rock R3)	1.0	5	8.8	43	0.3	2
Medium sandstone	1.0	2.7	0.25	43	0.3	2
Siltstone (Hard rock R2)	1.0	5	8.8	43	0.3	2
Medium sandstone	1.0	2.7	0.25	43	0.3	2
Sandy mudstone (Hard rock R1)	5.0	9	0.5	43	0.3	2
4-2 coal seam	1.0	2.7	0.5	39	0.3	2
Mudstone	10	27	1.3	38	0.4	2
Siltstone	1.0	5	8.8	43	0.3	2

pressure, and longitudinal tensile cracks begin to appear in the hard rock R2. When advancing to 150 m, the hard rock R2 bends and breaks, forming a “Voussoir beam” structure. The separation occurs, and the hard rock R3 breaks from the middle of the suspension area, showing a “Cantilever beam” state. At this time, the mining-induced fracture extends to the floor of 22 coal seam and connects with the water-conducting fracture zone of 22,108 working face, forming an ultra-high water-conducting fracture zone.

When advancing to 300 m, the numerical simulation mining is completed. At this time, the hard rock R3 is also broken, forming a “Voussoir beam” structure, which is not unstable under the support of the filling rock in the goaf. The floor failure range of the upper coal is connected with the development range of the lower coal falling zone, the gob area is compacted and the separation layer is closed. The high-level hard rock breaks along the cut-off and the stop line, resulting in obvious bending and existing in the form of a “Voussoir beam.” At this time, the height of the lower falling zone is 35.97 m, the ratio of mining to falling is 1:6 and the height of the water-conducting fractured zone is 184.57 m.

4.2 Analysis of development law of mining surface cracks

According to the theory and method of mining subsidence, coal mining ground cracks are mainly divided into boundary cracks and dynamic cracks. Boundary cracks are generally in the outer edge area of the stop line and cut-off. Dynamic cracks are located on the surface above the working face, parallel to the working face, and are continuously generated and closed as the working face advances (Hu et al., 2014). Based on elastic finite element theory, after coal mining, the stress distribution area of overlying strata can be divided into compressive stress area, tensile stress area, tensile stress area of positive curvature, compressive stress area of negative curvature, and supporting pressure area (Yang et al., 2019). Among them, the surface on both sides of the gob area belongs to the tensile stress area of positive curvature, and the surface above the goaf belongs to the compressive stress area of negative curvature.

With the first breaking of the main roof (working face advancing to 90 m), the longitudinal boundary cracks appeared on the surface for the first time. Since then, with the advancement of the working face, the mining boundary cracks appeared on the surface, and the boundary cracks are mainly vertical rock layer cracks, as shown in Figure 6, which is consistent with the research conclusion of Zhang Yujun (Zhang and Li, 2011). The first mining cracks are mainly boundary cracks. This is because the surface on both sides of the gob area is located in the tensile stress area, and the tensile strength of the surface loess overburden is almost negligible, which is easily damaged by tension under the influence of the goaf. The boundary crack of the cut-off behind the cut-off by 100 m and the average spacing of the cracks is 49 m. The boundary cracks of the stop line are 110 m ahead of the stop line, and the average spacing of the cracks is 34 m.

Compared with the first mining, surface damage is serious after repeated mining. As shown in Figure 7, after repeated mining, the boundary cracks develop to the position of the cut-off and stop line. The average spacing of boundary cracks of cut-off is 53.2 m, and that of the stop line is 38.7 m. The number of boundary cracks doubled, which is due to repeated mining caused by the extent of the roof bending damage, resulting in horizontal movement of surface soil to the gob area. Different from the first mining, after repeated mining, a “trapezoid” crack-intensive staggered area is formed at the surface position in the middle of the goaf. This is due to the increase of the longitudinal damage range of the overburden caused by repeated mining, resulting in the bending and sinking of the bedrock under

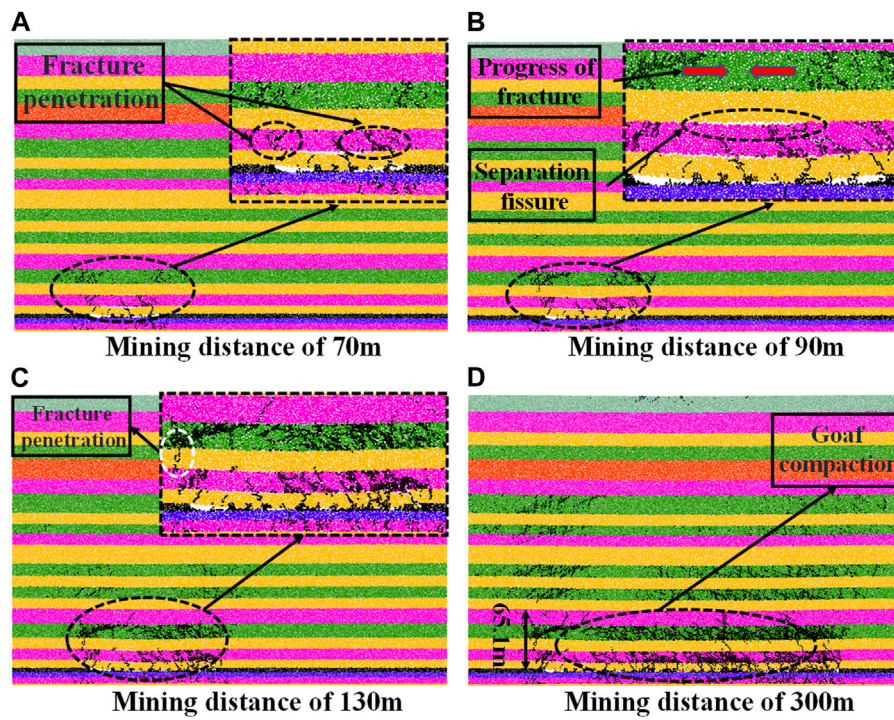


FIGURE 4
The first mining overburden structure evolution characteristic diagram. (A-D) show the mining distance of 70 m, 90 m, 130 m and 300 m, respectively.

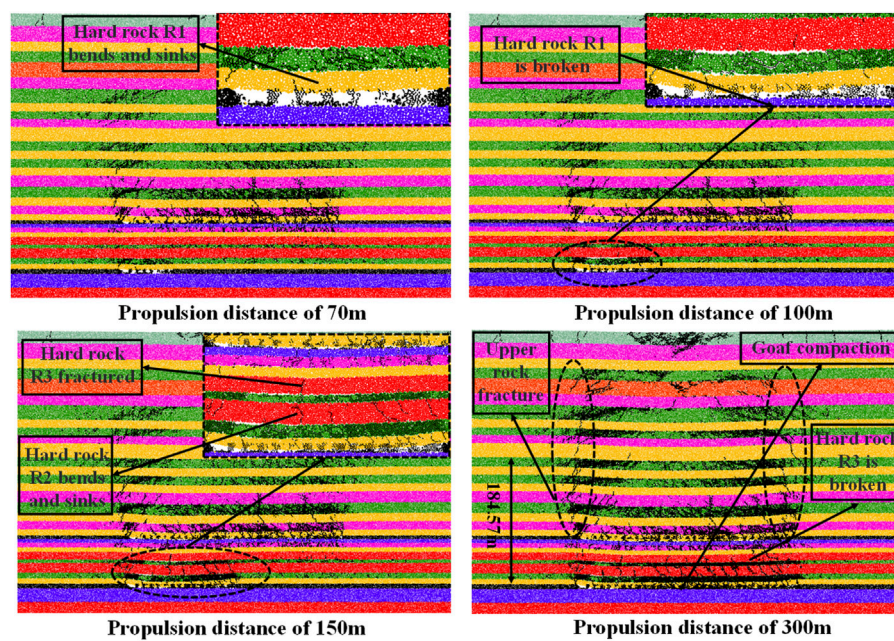


FIGURE 5
Overburden rock structure evolution characteristic diagram of repeated mining.

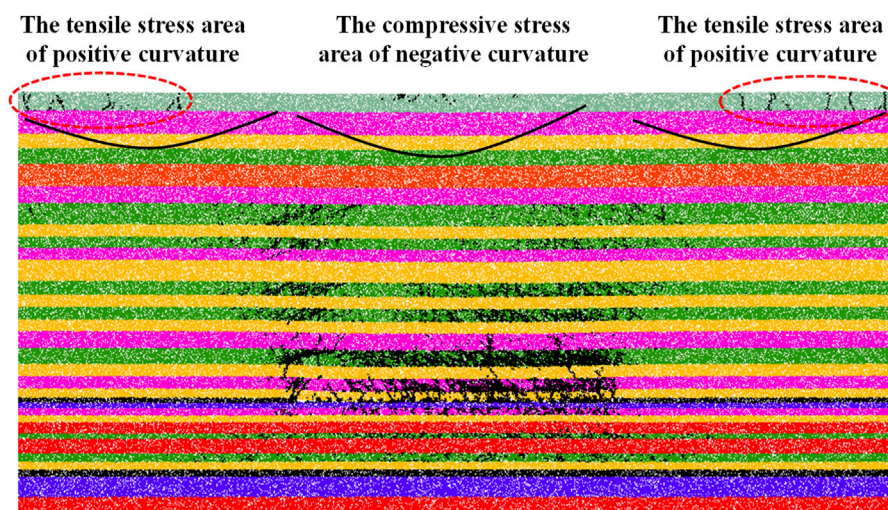


FIGURE 6
Development law diagram of surface cracks in the first mining.

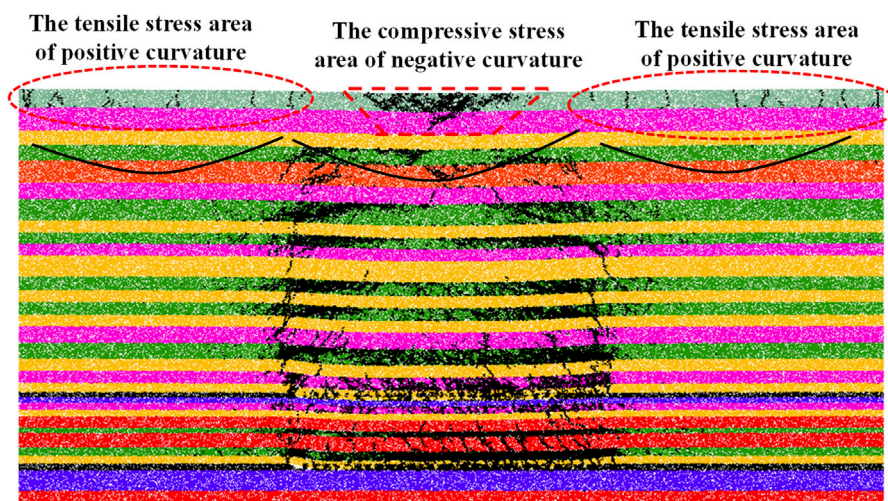


FIGURE 7
Surface crack development law diagram of repeated mining.

the loess overburden. The loess layer in the compressive stress area is destroyed by its own pressure, forming a dense compressive crack area.

4.3 Analysis of mining surface movement deformation

The planar position of the surface movement observation station is measured by GPS fast static method, and the level is measured by Leica DNA03s digital level. The layout of surface subsidence monitoring points in the 22,108 working face of Buertai Coal Mine is shown in Figure 8. There are 41 monitoring points in

the trend direction of the 22,108 working face, with a spacing of 20 m and a number of L06~L46. A total of 5 plane observations and 32 leveling and elevation observations were completed, and a large number of valuable observation data are obtained. The maximum surface subsidence is 2.209 m.

Numerical model after each step of excavation, compared with 22,108 working face surface subsidence monitoring point real point, every 20 m to set up a monitoring point, record the vertical displacement for statistical analysis, and draw a graph, as shown in Figure 9. Due to the influence of the adjacent goaf, the surface settlement curve monitored in the field is not symmetrical. The settlement value of the side adjacent to the goaf is relatively large. However, this is not the focus of this article, so it will not be described in detail.

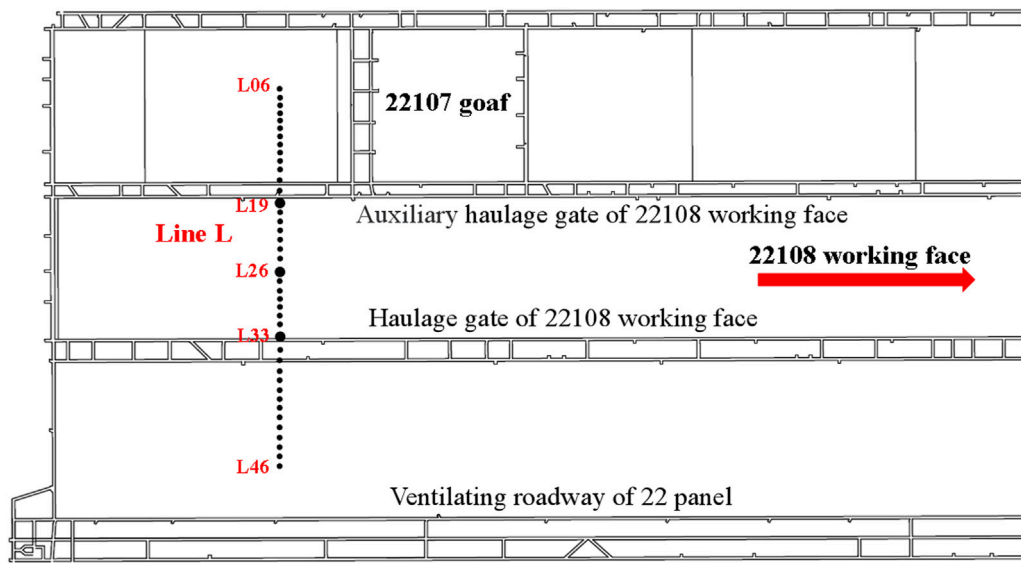


FIGURE 8
Twenty two thousand and one hundred and eight working face surface subsidence measuring point layout.

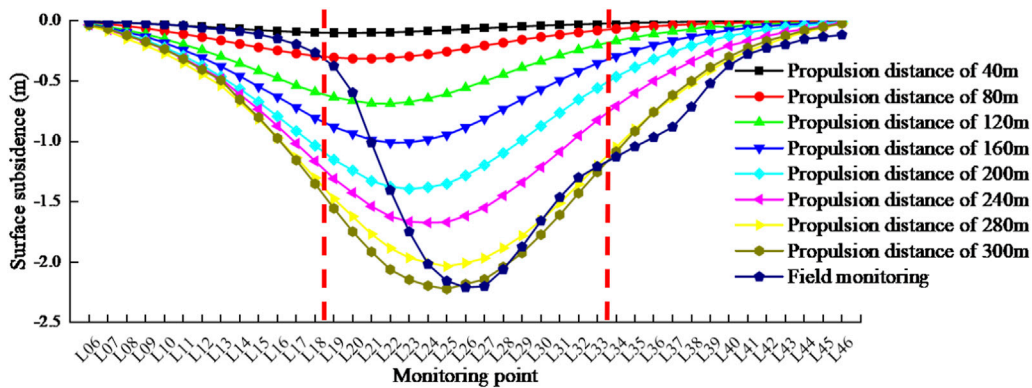


FIGURE 9
Vertical displacement characteristic diagram of first mining overburden.

During the mining process of the first mining face of 22,108, the surface settlement curve is a relatively gentle “bowl” shape. When the working face advances to 40, 80, 120, 160, 200, 240, 280, and 300 m, the maximum settlement is 0.099, 0.313, 0.687, 1.009, 1.393, 1.674, and 2.223 m respectively. With the continuous advancement of the working face, the range and amount of surface subsidence are increasing, the position of the maximum settlement is constantly moving to the right, and the settlement rate in the middle of the gob area is greater than that on both sides, finally, a relatively symmetrical subsidence basin is formed on the surface. The maximum subsidence of the surface is 2.22 m. The maximum subsidence position is located in the center of the goaf, which is slightly close to the direction of the cut-off, and the horizontal distance from the cut-off is 130 m. The surface subsidence trend of the 22,108 working face is the surface basin form of flat bottom, the

overall trend is relatively flat, the distance between the boundary of gob area and the edge of the basin bottom is large, and the slope is small, which is a typical feature of shallow buried deep collapse basin (Li et al., 2010).

The settlement curve of the numerical simulation of the 300 m mining is compared with the settlement curve of the 300 m advancing measured in the 22,108 fields. The numerical simulation results are basically consistent with the maximum settlement in the field measurement results, and the position of the maximum settlement in the numerical simulation is slightly left. In general, the numerical simulation results are basically the same as the field measurement, and the settlement trend conforms to the general law, which indicates that the process research and result analysis of overburden failure and surface movement caused by coal seam mining are credible.

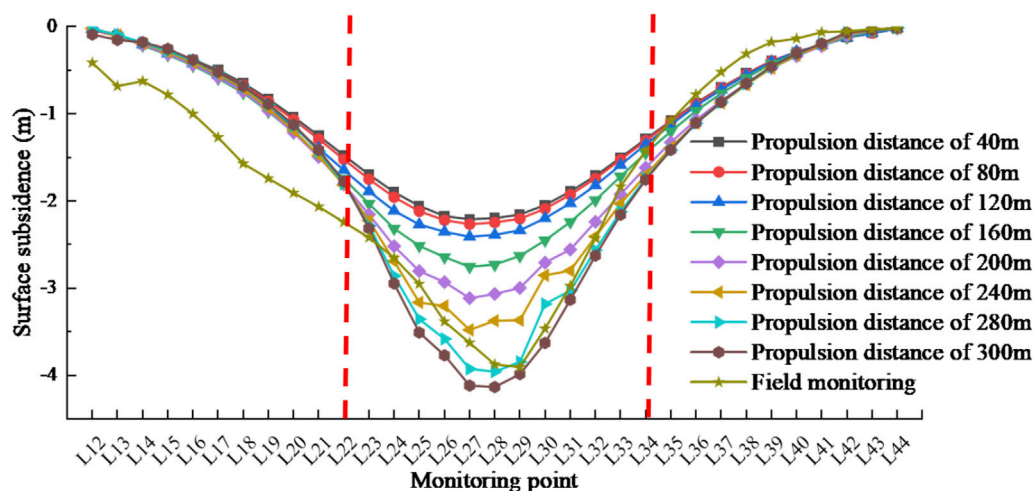


FIGURE 10
Vertical displacement characteristic diagram of repeated mining overburden rock.

During the mining process of the 42,108 repeated mining face, the surface subsidence curve is generally in a symmetrical “funnel” shape, with only one main inflection point. As shown in Figure 10, when the working face advances to 40, 80, 120, 160, 200, 240, 280, and 300 m, the maximum settlement is 2.209, 2.266, 2.410, 2.753, 3.112, 3.477, 3.955, and 4.132 m respectively. The position of the maximum settlement is stable in the direction of the central cutting hole of the 22,108 working face gob area. Compared with the first mining, the surface subsidence after repeated mining is significantly increased, and the maximum settlement is about 1.86 times the maximum settlement of the first mining. This shows that repeated mining changes the stable state of the broken roof of the upper coal seam, leading to the “activation” of the roof of the gob area, further aggravating the damage to the roof and even the surface.

The settlement curve of the numerical simulation of repeated mining 300 m is compared with the settlement curve of the 300 m measured in the 42,108 fields. The maximum settlement of the numerical simulation is 4.1 m, which is slightly larger than the 3.9 m measured in the field. The maximum settlement position of the numerical simulation is 20 m to the left.

4.4 Influence of panel incline width on overburden fracture

To study the influence of panel incline width on overlying rock strata failure law and surface fracture distribution, the mining overlying rock fracture and surface fracture distribution under the conditions of panel incline width of 340, 380, and 420 m are analyzed by using numerical simulation, respectively.

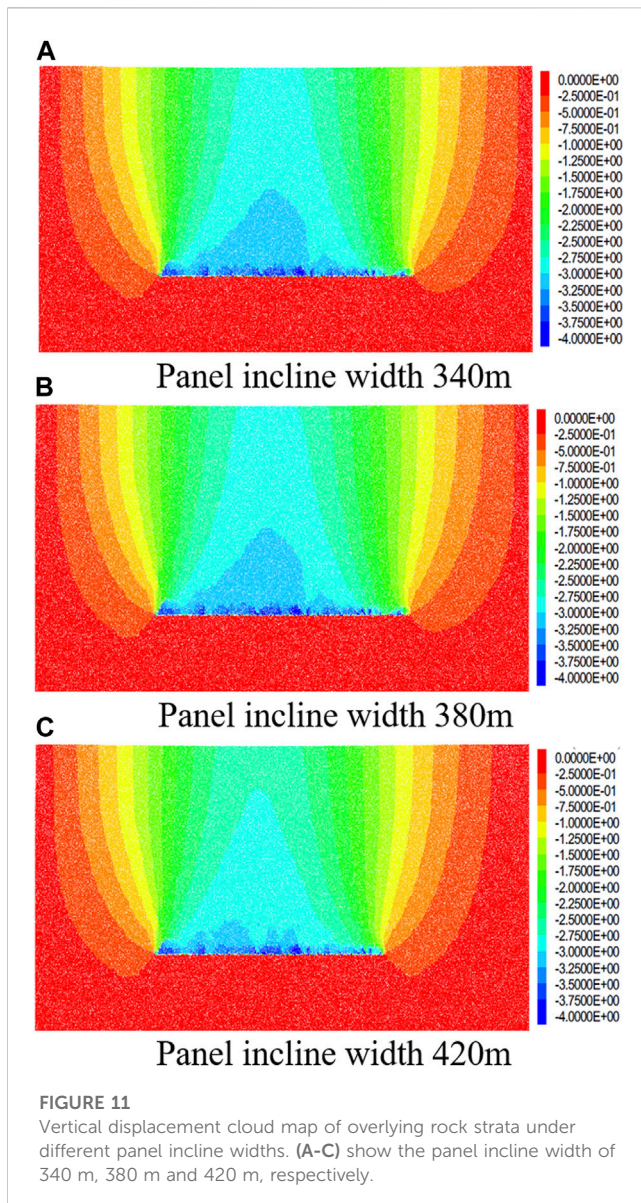
The selection of the panel incline width has a great influence on both the overlying rock strata and the surface, as shown in Figure 11. With the increase of the panel incline width, the influence range of the surface subsidence expands, especially

when the panel incline width exceeds 380 m. The surface subsidence of the goaf also increases with the increase of the panel incline width, and the surface subsidence basin is approximately “flat bottom” shape.

As can be seen from Figure 12, the increase of the panel incline width will lead to the increase of the area of the direct overhead, the bending of the basic roof and the formation of longitudinal cracks. Comparing the caving morphology and fracture propagation characteristics of overlying rock strata under three kinds of panel incline widths, the caving zone height is 21 m and does not increase with the increase of panel incline widths. The basic roof S2 still exists in the form of stable “masonry beam” and does not collapse, which is related to the geological characteristics of large basic roof thickness and high backfill degree of gob in Buertai coal mine. At the same time, with the increase of the panel incline width, the surface cracks did not change very much, and the cracks expanded laterally. In the longitudinal direction, due to the existence of high thick hard bedrock, the cracks did not expand upward after expanding to a certain height, and the height of the water-conducting fracture zone is 65.1 m.

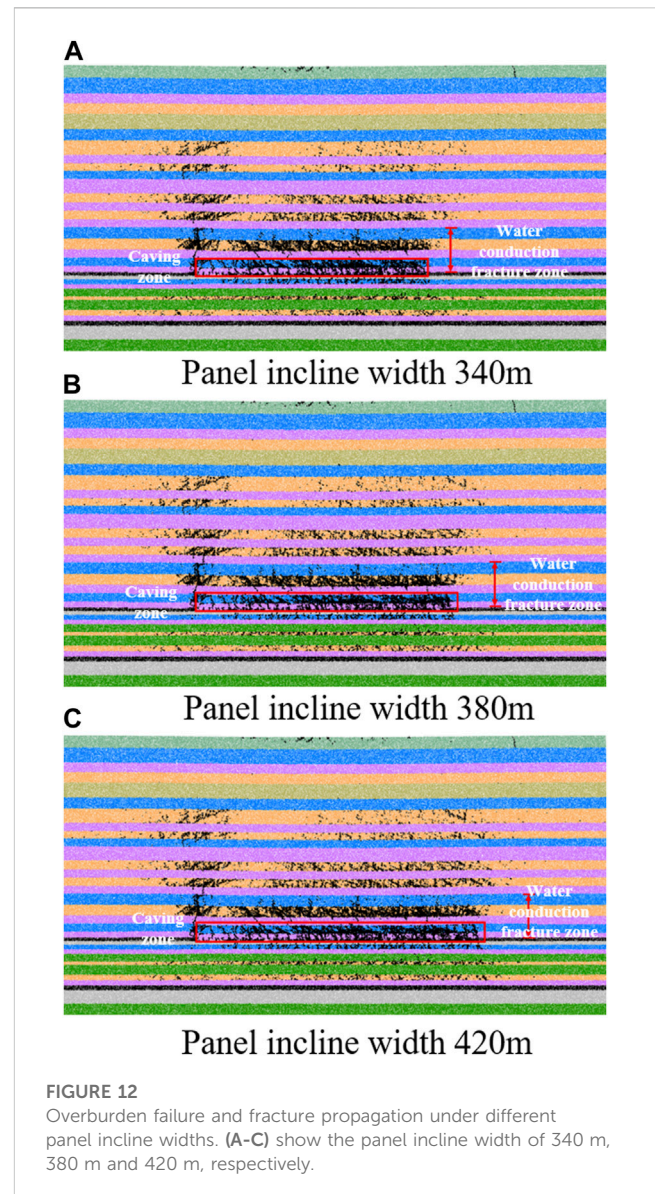
5 Discussion

With the expansion of the gob area, the movement range of overburden strata also expands, and the final movement range extends to the surface, causing surface movement and deformation. The surface subsidence is the result of the upward transmission of mining overburden strata. The lower coal seam mining activates the upper goaf, causing the “secondary damage” of the original damaged rock. The overlying strata of the upper gob area are broken again and deposited in the goaf in a loose state. Under the influence of secondary mining, the stress balance of overlying strata is also destroyed again, which leads to the instability and compaction of overlying strata in the previous gob area. Therefore, it will lead to



the surface subsidence above the gob area again, and the degree of subsidence is much greater than the first mining. The working face is covered with 12–18 m loess. Compared with the bedrock, loess has the characteristics of low density, low strength, and no tensile strength, which makes it easy to deform when subjected to external forces, and cannot form a supporting structure similar to a “beam.” Under its own pressure, it sinks with the sinking of bedrock.

Actually, the morphology of overburden fracture propagation caused by multi-seam mining is complex, and is related to many factors, including lithology, working face layout, mining speed, etc. The overburden migration prediction models for single coal seam mining are not applicable. However, From the illustration of a case study at Buertai Coal Mine, the overburden migration caused by mining multiple coal seams is not a simple superposition of the migration caused by each coal seam. The overburden structure disturbance caused by the previous coal seam and rock cracking—settlement have great influence on the mining of the latter coal seam.



6 Conclusion

In this paper, Taking the 22,108 and 42,108 working faces of Buertai Coal Mine as a research object, the surface subsidence monitoring technology and the discrete element method are used to simulate the migration and failure characteristics of overlying strata, and the propagation of cracks in the process of multi-coal seams mining is also been investigated. The conclusions are as follows:

- (1) After the exploitation of the lower coal seam, the water-conducting fractured zone develops upward and is connected with the fracture zone of the upper coal seam. Due to the large thickness of the basic roof of the coal seam in Buertai Coal Mine, resulting in a high backfilling height of the goaf, and the overlying hard layer is easy to form a “Voussoir beam” structure with bearing capacity;
- (2) So many cracks develop in the soft strata overlying the coal seam, and they cross each other and form a complex fracture

system. The hard layer is subjected to tensile action, resulting in crisscross cracks. The crack size is large, and they are mainly high-angle longitudinal cracks. In the process of single-layer mining, surface cracks are mainly longitudinal tensile cracks in the tensile stress area; after repeated mining, the compressive cracks in the surface compressive stress area are densely developed;

- (3) In Buertai Coal Mine, the surface subsidence curve of single coal seam mining shows a wide and slow “bowl” type, and the surface subsidence curve of double coal seam mining shows a “funnel” type with only one inflection point. The maximum surface subsidence position is located on the left side of the center of the working face and is consistent with the maximum subsidence position when single-layer mining;
- (4) The overburden migration caused by mining multiple coal seams is not a simple superposition of the migration caused by each coal seam. The overburden structure disturbance caused by the previous coal seam and rock cracking—settlement have great.

Data availability statement

The original contributions presented in the study are included in the article/Supplementary Material, further inquiries can be directed to the corresponding author.

Author contributions

JZ: Investigation, Writing—original draft, Funding acquisition. MW: Investigation, Writing—review and editing, Funding

References

- Adhikary, D., Khanal, M., Jayasundara, C., and Balusu, R. (2015). Deficiencies in 2d simulation: a comparative study of 2d versus 3d simulation of multi-seam longwall mining. *Rock Mech. Rock Eng.* 49, 2181–2185. doi:10.1007/s00603-015-0842-7
- Baek, J., Kim, S. W., Park, H. J., and Jung, H. S. (2008). Analysis of ground subsidence in coal mining area using SAR interferometry. *Geosciences J.* 12 (3), 277–284. doi:10.1007/s12303-008-0028-3
- Cho, N., Martin, C. D., and Segoo, D. C. (2007). A clumped particle model for rock. *Int. J. Rock Mech. Min. Sci.* 44, 997–1010. doi:10.1016/j.ijrmms.2007.02.002
- Ge, L., Chang, H. C., and Rizos, C. (2007). Mine subsidence monitoring using multi-source satellite SAR images. *Photogrammetric Eng. Remote Sens.* 73 (3), 259–266. doi:10.14358/pers.73.3.259
- Ghabraie, B., Ren, G., James, B., and John, V. (2017b). A predictive methodology for multi-seam mining induced subsidence. *Int. J. Rock Mech. Min. Sci.* 93, 280–294. doi:10.1016/j.ijrmms.2017.02.003
- Ghabraie, B., Ren, G., and Smith, J. V. (2017a). Characterising the multi-seam subsidence due to varying mining configuration, insights from physical modelling. *Int. J. Rock Mech. Min. Sci.* 93, 269–279. doi:10.1016/j.ijrmms.2017.02.001
- Ghabraie, B., Ren, G., Zhang, X., and Smith, J. (2015). Physical modelling of subsidence from sequential extraction of partially overlapping longwall panels and study of substrata movement characteristics. *Int. J. Coal Geol.* 140, 71–83. doi:10.1016/j.coal.2015.01.004
- Guoqing, Y., and Jingqin, M. (2008). D-InSAR technique for land subsidence monitoring. *Earth Sci. Front.* 15 (4), 239–243. doi:10.1016/s1872-5791(08)60059-7
- He, S., Xie, S., Song, B., Zhou, D., Sun, Y., and Han, S. (2016). Breaking laws and stability analysis of damage main roof in close distance hypogynous seams. *J. China Coal Soc.* 41 (10), 2596–2605.
- Hu, Z., Wang, X., and He, A. (2014). Distribution characteristic and development rules of ground fissures due to coal mining in windy and sandy region. *J. China Coal Soc.* 39 (01), 11–18.
- Itasca Consulting Group (2005). *Inc.Manual of particle flow code in 2-dimension*. Minneapolis: Itasca Consulting Group Inc. Version 3.10.
- Jung, H. C., Kim, S. W., Jung, H. S., Min, K. D., and Won, J. S. (2007). Satellite observation of coal mining subsidence by persistent scatterer analysis. *Eng. Geol.* 92 (1–2), 1–13. doi:10.1016/j.enggeo.2007.02.007
- Li, L., Tang, C., and Liang, Z. (2010). Investigation on overburden strata collapse around coal face considering effect of broken expansion of rock. *Rock Soil Mech.* 31 (11), 3537–3541.
- Liu, C., Li, H., and Mitri, H. (2019b). Effect of strata conditions on shield pressure and surface subsidence at a longwall top coal caving working face. *Rock Mech. Rock Eng.* 52, 1523–1537. doi:10.1007/s00603-018-1601-3
- Liu, Z., Zhong, X., Botao, Q., et al. (2019a). Redevelopment of fractures and permeability changes after multi-seam mining of shallow closely spaced coal seams. *Archives Min. Sci.* 64 (4).
- Liu, S. (2016). *The law of the overburden failure in thick coal seam mining and instability criterion of the clay aquiclude under the influence of mining[D]*. Beijing: China University of Mining and Technology.
- Liu, Y., Yang, T., Ye, Q., Hou, X., Zhao, Y., Wei, L., et al. (2022). Characteristics of surface deformation under repeated mining in mountainous area. *J. Min. Saf. Eng.* 39 (03), 507–516.
- Ma, W. J., and Hu, H. F. (2013). The strata movement regularity and parameter simulation analysis in multiple seams repeated mining. *Appl. Mech. Mater.* Trans Tech Publications Ltd 295, 2935–2939. doi:10.4028/www.scientific.net/amm.295-298.2935
- Perski, Z., Hanssen, R., Wojcik, A., and Wojciechowski, T. (2009). InSAR analyses of terrain deformation near the Wieliczka Salt Mine, Poland. *Eng. Geol.* 106 (1–2), 58–67. doi:10.1016/j.enggeo.2009.02.014
- Wang, G., Wu, M., Wang, R., Xu, H., and Song, X. (2017). Height of the mining-induced fractured zone above a coal face. *Eng. Geol.* 216, 140–152. doi:10.1016/j.enggeo.2016.11.024

acquisition. LB: Methodology, Writing—review and editing. CY: Writing—review and editing, Software.

Funding

The authors declare financial support was received for the research, authorship, and/or publication of this article. This work was supported by Open Fund of the State Key Laboratory of Water Resource Production and Utilization in Coal Mining (No. WPUKFJJ 2019-18), and Education science and technology research plan guiding project of Hubei Provincial Department (No. B2021272), and Wuhan Knowledge innovation special project (No. 2022010801020429).

Conflict of interest

The authors declare that the research was conducted in the absence of any commercial or financial relationships that could be construed as a potential conflict of interest.

Publisher's note

All claims expressed in this article are solely those of the authors and do not necessarily represent those of their affiliated organizations, or those of the publisher, the editors and the reviewers. Any product that may be evaluated in this article, or claim that may be made by its manufacturer, is not guaranteed or endorsed by the publisher.

- Wang, J., Wei, W., Zhang, J., and Mishra, B. (2020). Numerical investigation on the caving mechanism with different standard deviations of top coal block size in LTCC. *Int. J. Min. Sci. Technol.* 30 (5), 583–591. doi:10.1016/j.ijmst.2020.06.001
- Wei, J., Wang, S., Song, S., Sun, Q., and Yang, T. (2022). Experiment and numerical simulation of overburden and surface damage law in shallow coal seam mining under the gully. *Bull. Eng. Geol. Environ.* 81 (5), 207. doi:10.1007/s10064-022-02706-y
- Wu, T., Zhang, H., Wang, C., Tang, Y., and Wu, H. (2008). Retrieval of urban slow deformation using the multi-baseline DInSAR technique. *Chin. Sci. Bull.* 53 (23), 3705–3714. doi:10.1007/s11434-008-0331-4
- Yang, X., Wen, G., Dai, L., Sun, H., and Li, X. (2019). Ground subsidence and surface cracks evolution from shallow-buried close-distance multi-seam mining: a case study in Bulianta coal mine. *Rock Mech. rock Eng.* 52 (8), 2835–2852. doi:10.1007/s00603-018-1726-4
- Yang, Y. U., Shen, W., and Gao, J. (2016). Deformation mechanism and control of lower seam Roadway of contiguous seams. *J. Min. Saf. Eng.* 33 (01), 49–55.
- Yao, B., Zhou, H., and Chen, L. (2010). Numerical simulation about fracture development in overlying rocks under repeated mining. *J. Min. Saf. Eng.* 27 (03), 443–446.
- Zhang, J., and Li, Y. (2019). Coal strength development with the increase of lateral confinement. *Energies* 12 (3), 405. doi:10.3390/en12030405
- Zhang, Q., Zou, J. P., Wang, J., Jiao, Y. Y., and Xu, H. (2023a). Mechanism of coal bump induced by joint slipping under static and dynamic stresses in graben structural area. *Acta Geotech.* doi:10.1007/s11440-023-01947-9
- Zhang, Q., Zou, J. P., Wu, K. B., et al. (2023b). On the characteristics of mine earthquakes induced by key strata breaking during deep mining. *Chin. J. Rock Mech. Eng.* 42 (5), 1150–1161.
- Zhang, X., Ghabraie, B., Ren, G., and Tu, M. (2018). Strata movement and fracture propagation characteristics due to sequential extraction of multiseam longwall panels. *Adv. Civ. Eng.* 2018, 1–17. doi:10.1155/2018/4802075
- Zhang, Y., and Li, F. (2011). Monitoring analysis of fissure development evolution and height of overburden failure of high tension fully-mechanized caving mining. *Chin. J. Rock Mech. Eng.* 30 (1), 2994–3001.
- Zhao, Y., Wang, X., Guo, Y., Danesh, N. N., and Jiang, Y. (2022). Mechanical properties and brittleness characteristics of sandstone from different burial depths. *Geomechanics Geophys. Geo-Energy Geo-Resources* 8 (5), 165. doi:10.1007/s40948-022-00470-7
- Zou, J., Hu, X., Jiao, Y. Y., Chen, W., Wang, J., Shen, L. W., et al. (2022b). Dynamic mechanical behaviors of rock's joints quantified by repeated impact loading experiments with digital imagery. *Rock Mech. Rock Eng.* 55 (11), 7035–7048. doi:10.1007/s00603-022-03004-5
- Zou, J., Wu, K., Zhang, X., Zhu, J., Zhou, Z., Zheng, F., et al. (2022a). Effective evaluation of deep-hole blasting for controlling strong tremors induced by deep coal mining-A case study. *Int. J. Rock Mech. Min. Sci.* 159, 105211. doi:10.1016/j.ijrmms.2022.105211